addition has no direct effect on shear layer instability. The entropy wave s' does depend on Q', but may be computed via Eq. (3) after obtaining $\boldsymbol{u}'$ and p'.

It may be noted that formulations using either thermodynamic or kinematic definitions of sound lead to the same result for the case of a vanishing time-dependent component of the heat addition rate. Using the thermodynamic definition, acoustic waves are suppressed by neglecting the pressure perturbation in the equation of state so that

$$\bar{T}\rho' + \bar{\rho}T' = 0 \tag{8}$$

Then, utilizing the linearized continuity and energy equations (with no time-dependent heat source) results in the condition that the velocity oscillations are divergence free, which recovers Eq. (7). The linearized momentum equation is still given by Eq. (6) so that the correspondence with the suppression of acoustic waves using the kinematic definition of sound is complete for this case.

Acknowledgment

This work was supported by NASA Lewis Research Center under Contract NAS3-25266.

References

[1]Shin, D. S., and Ferziger, J. H., "Linear Stability of the Reacting Mixing Layer," *AIAA Journal*, Vol. 29, No. 10, 1991, pp. 1634–1642.

[2]Mahalingam, S., Cantwell, B. J., and Ferziger, J. H., "Stability of Low-Speed Reacting Flows," *Physics of Fluids A*, Vol. 3, No. 6, 1991, pp. 1533–1543.

[3]Mahalingam, S., "Numerical Solution of the Viscous Stability Equations for Low-Speed Reacting Flows," *International Journal for Numerical Methods in Fluids*, Vol. 15, 1992, pp. 729–741.

[4]Planche, O. H., and Reynolds, W. C., "Heat Release Effects on Mixing in Supersonic Reacting Free Shear-Layers," AIAA Paper 92-0092, Jan. 1992.

[5]Yates, J. E., and Sandri, G., "Bernoulli Enthalpy: A Fundamental Concept in the Theory of Sound," *Aeroacoustics: Jet Noise, Combustion and Core Engine Noise*, edited by I. R. Schwarz, Massachusetts Inst. of Technology Press, Cambridge, MA, 1976, pp. 65–89.

[6]Yates, J. E., "Application of the Bernoulli Enthalpy Concept to the Study of Vortex Noise and Jet Impingement Noise," NASA CR 2987, April 1978.

[7]Hegde, U. G., and Zinn, B. T., "Vortical Mode Instability of Shear Layers with Temperature and Density Gradients," *AIAA Journal*, Vol. 28, No. 8, 1990, pp. 1389–1396.

Long Distance Propagation Model and Its Application to Aircraft En Route Noise Prediction

Kingo J. Yamamoto* and Michael J. Donelson†

McDonnell Douglas Aerospace—Transport Aircraft, Long Beach, California 90846

Introduction

As a member of the SAE A-21 Aircraft Noise Committee En Route Noise Group, McDonnell Douglas Aerospace (MDA) participated in the Aircraft En Route Noise Technology Program developed by NASA/FAA. As part of the research activities of this program, two en route noise tests were conducted, one in Madison and Limestone Counties, Alabama in 1987, and the other in White Sands Missile Range, New Mexico in 1989. These tests were designed to address the atmospheric propagation of advanced turboprop noise from cruise altitudes.

Received March 30, 1993; revision received June 2, 1993; accepted for publication June 2, 1993. Copyright © 1993 by the American Institute of Aeronautics and Astronautics, Inc. All rights reserved.

*Principal Scientist, Acoustics Technology, 3855 Lakewood Blvd.

†Engineer, Acoustics Technology, 3855 Lakewood Blvd.

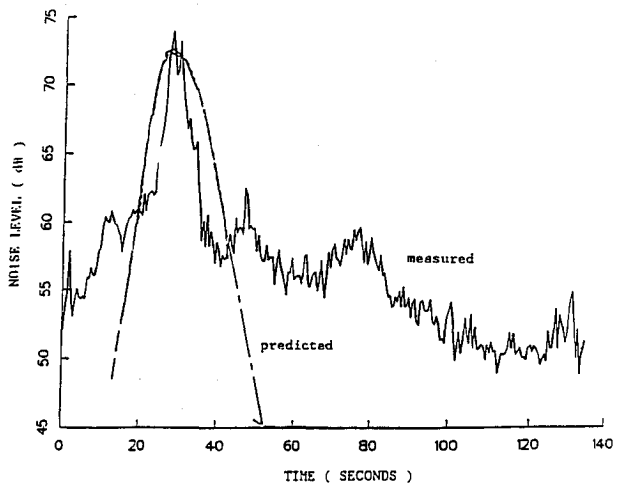

Fig. 1 Comparison of measured and predicted en route noise time histories: run 202, flight altitude = 4.6 km (15,000 ft), BPF = 233 Hz.

During this period, MDA developed a three-dimensional long distance propagation model designed to be used exclusively for en route noise prediction. In this paper the structure of the model is outlined, and its applications to en route noise predictions are also discussed.

Theoretical Background

The long distance propagation model presented here was developed based on the ray theory of Ref. 1. The model is designed to be used exclusively for aircraft en route noise prediction in the stratified atmosphere. Two major assumptions were adopted in this model: 1) The atmosphere-related parameters such as pressure, temperature, wind velocity, and humidity should not change appreciably in the vertical direction over the wavelength of the sound whose propagation is in concern. 2) The vertical component of the wind velocity is negligibly small. Then, the governing equations for the long distance propagation are written as

$$\begin{aligned}
x(z) &= x_0 + \int_{z_0}^{z} [c(z)^2\sigma_x + \{1 - [v_x(z)\sigma_x + v_y(z)\sigma_y]\} \\
&\quad \times v_x(z)\,]\,[c(z)^2\sigma_z(z)]^{-1}\,dz \\
y(z) &= y_0 + \int_{z_0}^{z} [c(z)^2\sigma_y + \{1 - [v_x(z)\sigma_x + v_y(z)\sigma_y]\} \\
&\quad \times v_y(z)\,]\,[c(z)^2\sigma_z(z)]^{-1}\,dz \\
\sigma_x &= \cos\theta\{c(z_0) + v_x(z_0)\cos\theta + v_y(z_0)\sin\theta\cos\phi\}^{-1} \\
\sigma_y &= \sin\theta\cos\phi\{c(z_0) + v_x(z_0)\cos\theta + v_y(z_0)\sin\theta\cos\phi\}^{-1} \\
\sigma_z(z) &= [c(z)^{-2}\{1 - (v_x(z)\sigma_x + v_y(z)\sigma_y)\}^2 \\
&\quad - (\sigma_x^2 + \sigma_y^2)\,]^{0.5} \\
x_0 &= R\cos\theta \\
y_0 &= R\sin\theta\cos\phi \\
z_0 &= R\sin\theta\sin\phi
\end{aligned} \tag{1}$$

where the positive x corresponds to flight direction, and the z axis is taken to be normal to the ground whose positive sense is downward. The polar and azimuthal angles θ and ϕ are measured from the positive x axis and the positive y axis to the ray, respectively. The term $c(z)$ is the local speed of sound at z, and $Vx(z)$ and $Vy(z)$ are the x and y component of wind velocity at z, respectively.

The Blokhintzev invariant which implies conservation of energy flux for a given ray tube may be written as

$$\frac{P(z)^2 A(z)\{[v_x(z)+s(z)\sigma_x]^2+[v_y(z)+s(z)\sigma_y]^2+\sigma_z(z)^2\}}{\{1-[v_x(z)\sigma_x+v_y(z)\sigma_y]\}\rho(z)c(z)^2}=\text{const} \tag{2}$$

$$s(z)=c(z)\{1-[v_x(z)\sigma_x+v_y(z)\sigma_y]\}^{-1}$$

The constant on the right hand side can be determined with the boundary conditions at the reference wave front, where source strength is known. $A(z)$ is the ray tube cross-sectional area normal to the ray.

The stratified medium is divided into n slabs when the model is applied to the sound propagation in the atmosphere. In each slab the sound speed is assumed to be constant and to jump to a different value at the interface between slabs. The energy reflected back from the interface is inversely proportional to the square of number of slabs. Hence, by increasing the number of slabs, we can make the energy loss due to reflection negligibly small.[2]

Sound propagation in air undergoes absorption by air mainly due to the vibrational relaxation process of air molecules. This mechanism is well understood, and the calculation method for the absorption is also well established. In the present model, the American National Standards Institute (ANSI) method[3] is employed to address this issue. The total attenuation due to the absorption is then calculated by applying the ANSI method to Doppler-shifted frequencies over the entire ray trajectory.

Application to En Route Noise Prediction

The long distance propagation model discussed was applied to the prediction of aircraft en route noise predictions. Predictions were compared with the data from the En Route Noise Test conducted at the White Sands Missile Range, New Mexico in 1989. (Details of the test program are found in Ref. 4.)

In this test, NASA's Gulfstream II was used as a test airplane. An eight-bladed SR-7L single rotation propeller was mounted on its wing. The source strength was determined by the microphones on a chase airplane (Learjet). Sound pressure levels for the blade passing frequency (BPF) and higher harmonics were measured when the source airplane was at cruise at the nominal altitudes of 4.6 km (15,000 ft) and 9.2 km (30,000 ft) and at flight Mach numbers of 0.5 (at the altitude of 4.6 km) and 0.7 (at the altitudes of 4.6 and 9.2 km).

An array of eight microphones measured en route noise for 88 runs which were performed at the altitudes of 4.6 km and 9.2 km. Time histories of overall sound pressure levels were obtained from the ensemble-averaged data. The meteorological profiles were measured with a tethered balloon and a free released radiosonde balloon during the test from ground level up to 12 km. The coordinates of the source airplane were determined by the tracking radar for approximately every 0.1 s over 90-s duration.

Prediction of en route noise based on Eqs. (1) and (2) is made in the following steps: 1) Extrapolate source noise SPL directivity to that at 100 m. 2) Interpolate meteorological data from ground level up to the source altitude for every 1 m which corresponds to the layer thickness. 3) Determine the ray trajectory for a given set of source and monitor locations with Eq. (1) (in this step, the polar and azimuthal angles for the corresponding emission direction are determined). 4) Determine Doppler-shifted frequency to be observed by the monitor on the ground with the source noise frequency, flight Mach number, and corresponding emission angle. 5) Determine the sound attenuation due to air absorption by applying the ANSI method to the Doppler-shifted frequency over the ray trajectory determined in step 3. 6) Determine the sound attenuation due to the spherical divergence by Eq. 2. 7) Determine the sound pressure levels at the monitor location by subtracting the attenuations of steps 5) and 6) from source strength. 8) Determine the sound pressure level time history. (Using the radar tracking data, we were able to determine the flight elapsed time from the reference point, which corresponds to the time when sound recording was initiated, to a give flyover point.)

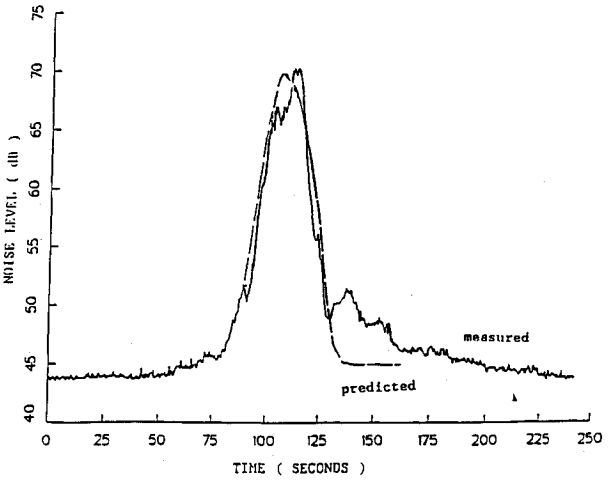

Fig. 2 Comparison of measured and predicted en route noise time histories: run 307, flight altitude = 4.6 km (15,000 ft), BPF = 232 Hz.

In the present data-to-prediction comparison, two cases were selected from the En Route Noise Test Program, which are run 202 and run 307. The criterion for this selection was that the projected flightpath on the ground should be in line with the microphone array as closely as possible. It should be noted that in these sample comparisons the predicted noise level is only for the BPF whereas the measured data is for the total noise including BPF and its higher harmonics.

1) Run 202: Flight altitude and flight speed for this run was 4.6 km and 207 m/s, respectively. Figure 1 presents the time history comparison for this run. The BPF is 233 Hz. The weather data used for this prediction were recorded approximately 2 h after the flight. We note that the peak location is accurately predicted but its level is slightly lower than measured peak. We also note that the measured data falls off much faster than prediction.

2) Run 307: Flight altitude and flight speed for this run was 4.6 km and 162 m/s, respectively. Figure 2 shows a similar time history comparison for this run. The BPF is 232 Hz. The weather data for this run were obtained approximately $1\frac{1}{2}$ h before the flight. We note an excellent agreement in both peak level and its location. We think that because of the long propagation distance higher harmonics undergo much larger absorption than BPF, and, therefore, they may not significantly contribute to the total noise.

In addition to the two cases presented, we made several similar data-to-prediction comparisons for higher altitude cases. The results were encouraging. However, for these cases we applied the ANSI method beyond its valid limitation. According to Ref. 3, the validity of the ANSI method has not been tested for the temperatures below $-40°C$. The weather data used for the calculation of these predictions show that the ambient temperature falls below $-40°C$ at the altitude of 6 km (20,000 ft) and above. For this reason, the results for higher altitudes are not presented herein.

Conclusions

A three-dimensional long distance propagation model was developed based on the ray theory. The model was tested against propfan en route noise test data. The source strength of propfan determined with chase plane microphones was extrapolated by the model to the ground and then compared with en route noise measured on the ground. The comparison indicated an excellent agree-

ment between measured and predicted data for both magnitude and location of the peak. It appears that en route noise level of the single rotation propeller is primarily determined only by the blade passing frequency at high altitude cruise missions.

Acknowledgments

This work was performed under the Independent Research and Development Program at McDonnell Douglas Aerospace—Transport Aircraft. The authors would like to express their sincere gratitude to William L. Willshire Jr. of NASA Langley Research Center and Donald P. Garber of Lockheed Engineering and Sciences Co. for providing us with PTA en route noise data.

References

[1]Pierce, A. D., *Acoustics*, McGraw-Hill, New York, 1981, pp. 371–419.

[2]Dowling, A. P., Ffowcs Williams, J. E., *Sound and Sources of Sound*, Ellis Horwood, Manchester, England, 1983, pp. 104–105.

[3]Anon., American National Standard, ANSI S1.26-1976, 1976.

[4]Willshire, W. L., Jr., Garber, D. P., "En Route Noise Test Preliminary Results," *Proceedings of International Conference on Noise Control Engineering*, Vol. 1, (Newport Beach, CA), Noise Control Foundation, Poughkeepsie, NY, Dec. 1989, pp. 309–312.

Three-Dimensional Laminar Boundary Layer in a Constant Pressure Diverging Flow—Blasius Equivalent

O. N. Ramesh,* J. Dey,† and A. Prabhu‡
Indian Institute of Science, Bangalore 560012, India

Introduction

ALTHOUGH a variety of three-dimensional (3D) laminar boundary layer problems have been addressed in the past, we consider here the development of a laminar boundary layer under streamline divergence but constant pressure. This interesting problem has arisen out of an experiment designed[1] to study the effect of streamline divergence, among other parameters associated with general 3D flows, on transitional flow characteristics. The streamline divergence effect under constant pressure is achieved[1,2] by modifying the wind tunnel. As shown in Fig. 1, a distorted section is created with one diverging side wall and a converging roof, thus providing lateral streamline divergence under constant pressure in the region of measurements made on a flat plate. A few typical surface streamlines from flow visualization study[2] are also shown in Fig. 1. Also it was reported that there was no skewing between the surface streamlines and those outside the boundary layer.[2]

The relevance of the present problem, apart from being basic in nature, is seen in the divergent channel flow, albeit with pressure gradient. Kehl,[3] for example, studies turbulent flow in a divergent channel, using a momentum integral method. Kehl[3] considers the flow to emanate from a fictitious source and further considers the flow along a streamline. Along a streamline the spanwise velocity is zero, but its spanwise derivative, which appears in the continuity equation, is nonzero. Thus the boundary layer momentum equation along a streamline is the same as that in 2D flow; however the 3D effect is introduced through the continuity equation.

Received April 16, 1993; accepted for publication April 24, 1993.
Copyright © 1993 by the American Institute of Aeronautics and Astronautics, Inc. All rights reserved.

*Research Scholar, Department of Aerospace Engineering.
†Assistant Professor, Department of Aerospace Engineering.
‡Associate Professor, Department of Aerospace Engineering.

Analysis

For the flow under consideration—streamline divergence under constant pressure—we also assume the flow to emanate from a source and consider the flow along a streamline direction (x). As shown in Fig. 2, the source is located at a distance A upstream of the origin of coordinates (x, z); z is the coordinate spanwise to x. The normal direction to the plate is denoted by y. Note that because this is a streamline based coordinate system, it changes from streamline to streamline.

Under the boundary layer approximation the continuity and momentum equations for the flow in the distorted duct with zero pressure gradient are[3]

$$u_x + v_y + u/(A + x) = 0 \tag{1}$$

$$uu_x + vu_y = \nu u_{yy} \tag{2}$$

where u and v denote, respectively, the velocities in x and y directions, ν denotes the kinematic viscosity, and subscripts x and y denote partial derivatives with respect to x and y, respectively. Note that the term $u/(A + x)$ in the continuity Eq. (1) corresponds to the z-derivative of the spanwise velocity component from a kinematical consideration. The boundary conditions for Eq. (2) are

$$\begin{aligned} u = v = 0 \quad &\text{at} \quad y = 0 \\ u \to U \quad &\text{as} \quad y \to \infty \end{aligned} \tag{3}$$

where U denotes the free-stream velocity along a streamline.

To solve Eqs. (1-3), we seek a similarity solution in terms of the similarity variables

$$\eta = y/\delta(x) \qquad u = Uf'(\eta) \tag{4}$$

where $\delta(x)$ is a measure of the local boundary layer thickness, and prime denotes derivative with respect to η.

With v from Eq. (1) and Eq. (4) as

$$v = U(\mathrm{d}\delta/\mathrm{d}x)[\eta f' - f] - [Uf\delta/(A + x)] \tag{5}$$

the momentum Eq. (2) becomes

$$f''' + ff''\{U\delta(\mathrm{d}\delta/\mathrm{d}x)/\nu + U\delta^2/[\nu(A + x)]\} = 0 \tag{6}$$

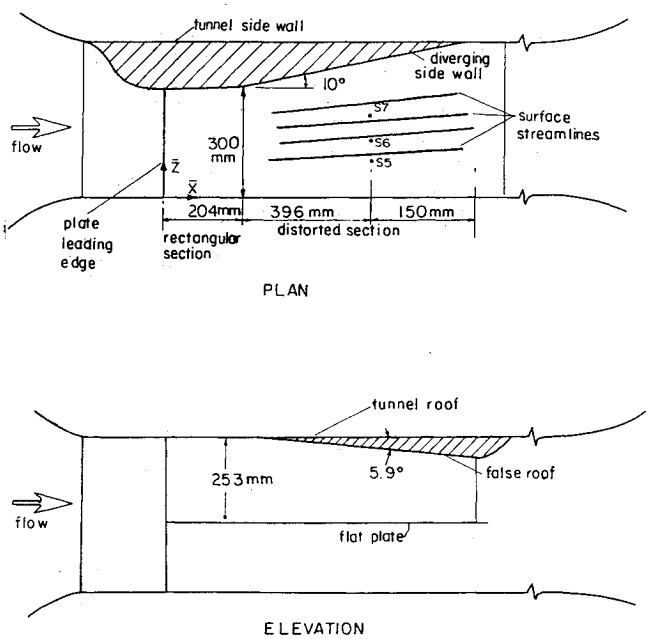

Fig. 1 Schematic view of the distorted test section with a few typical surface streamlines and measuring stations.